Ultimate Capacity Analysis of Orbital Angular Momentum Channels

Ashwini Sawant, Ingeun Lee, Bang Chul Jung, and EunMi Choi

Abstract

Orbital angular momentum (OAM) multiplexing has recently been proposed as a solution to the ultimate goal of increasing the channel capacity of wireless communication links because of the existence of infinite orthogonal modes. It can be combined with the existing conventional multiplexing techniques to boost up the data rate multiple times for future wireless communication systems. We analyze the fundamental behavior of the channel capacity of OAM channels based on two concepts for the most common Laguerre-Gaussian OAM beams: paraxiality and orthogonality. We also confirm our general theory by applying the proposed method to the evanescing OAM beams, circular transverse electric beams. Our study is based on calculating the paraxial estimator of these OAM beams and relating it as a parameter that limits the degree of freedom in OAM channels. In particular, we investigate the dependency on physical parameters, such as transmitter and receiver sizes, in our calculation to define the capacity of OAM channels.

Introduction

Recently, data transmission at higher data rates in wireless communication systems has been an ever-increasing demand owing to the global usage of smart technologies, including smartphones and Internet-of-Things (IOT) devices. This sets up an ambition for multifold increments in data rates with the onset of 5G wireless networks. To meet this demand, researchers are continuously looking for unconventional methods to boost data rates, by exploring novel radio resources, because conventional radio resources, such as frequency, time, and space, are almost doomed to be exhausted.

The fact that light beams can carry orbital angular momentum (OAM) was proved using Laguerre-Gaussian (LG) laser modes in 1992 [1]. These modes have well-defined OAM equal to $l\hbar$ per photon, where l denotes the azimuthal mode index and $\hbar$ denotes the reduced Planck's constant. This property of well-defined OAM is not only limited to LG modes, but more generally, can be found in any beam that follows $e^{il\phi}$ phase variation along the azimuthal angle. OAM beams are characterized by zero intensity, an indefinite phase at the axis, and a twisted helical phase front $e^{il\phi}$. Recently, the scientific community has shown a profound interest in OAM beams due to their wide applications in various research fields, including quantum physics, astronomy, optical trapping, and communication [2]. Considerable research has been carried out in the field of RF communication to increase the data rate with OAM multiplexing besides other multiplexing techniques. OAM multiplexing supports line-of-sight (LoS) communication and can be used for beyond-5G wireless backhaul links. Figure 1 shows a graphical representation of the wireless backhaul evolution using OAM beams. Several small cell base stations (SBSs) have been set up, which use the backhaul link to transfer the data to/from macro base stations (MBSs). Backhaul link is implemented with LoS mm-wave OAM beams to achieve high-speed data traffic. An OAM-based wireless backhaul link using the millimeter wave (mm-wave) spectrum exhibits high capacity, high directivity, and lower interference, compared to microwave and sub-6 GHz spectrum and can be used effectively in dense urban areas to provide both real-time and non real-time services [3]. Although it can be limited by the higher atmospheric attenuation, as well as turbulence, its potential would become immense if it can be successfully transmitted to longer distances in the turbulence-prone medium, such as air or sea, using the turbulence effect mitigation techniques [4].

OAM multiplexing is achieved by transmitting the information signals using the OAM modes of different orders, which are orthogonal to each other and can carry information on a channel without interference. It is envisioned as a supporting infinite degree of freedom (DoF) and an infinite channel capacity for free-space LoS communication in optical and radio frequency (RF) channels. However, it has long been argued that OAM multiplexing can provide infinite channel capacity, because the OAM modes can be generated with infinite order without disrupting their orthogonality property, irrespective of the transmitter and receiver sizes. This claim of infinite capacity is still under debate [5], and no clear general theories have yet emerged. Nonetheless, OAM multiplexing is still a potential candidate for overcoming the limit of the existing wireless communication technology. Additionally, OAM communication also has a drawback of high divergence, alignment issues and a lack of ease to generate the higher-order OAM beams.

Various research works carried out earlier to determine the practical channel capacity limitation of the OAM wireless communication in free

Digital Object Identifier:
10.1109/MWC.001.2000258

Ashwini Sawant, Ingeun Lee, and EunMi Choi are with Ulsan National Institute of Science and Technology (UNIST); Bang Chul Jung is with Chungnam National University.

1536-1284/21/$25.00 © 2021 IEEE

space [6, 7] were specifically focused on the conventional LG beams. In this article, we determine the DoF calculation of the OAM wireless communication link with a novel approach by introducing the most generalized physical quantities: paraxiality and orthogonality for generalized free-space OAM modes. This analysis is based on the key physical characteristic of OAM modes that are solutions of the Helmholtz equation with paraxial condition, and applicable to practical sizes of transmitter/receiver antennas and the propagation distances. In this article, we present novel formalism of OAM wireless channel DoF analysis and its simulation and experimental verification for conventional LG and evanescent circular transverse electric (TE) beams.

Paraxial Estimator for Free-Space OAM Communications

The infinite DoF of an OAM channel in free space is guaranteed when the paraxiality and orthogonality conditions are satisfied. We will discuss the paraxiality condition in this section. The solution to the Helmholtz equation with paraxial approximation in free space is an LG beam [1]. This beam is azimuthally symmetric in amplitude with zero intensity at the axis and its phase has a vorticity that depends on the order l.

Paraxial approximation simplifies the Helmholtz equation considering that the field is the product of the fast oscillatory part and a slowly varying complex amplitude. In addition, the variation of the complex amplitude along the propagation direction (z) over a distance comparable to wavelength, as well as its variation in the axial propagation direction, is small compared to that in the perpendicular direction. In situations where these conditions are not met, that is, the complex amplitude of the field is oscillating at a similar speed with the fast-oscillatory part, the paraxial approximation fails to provide the correct solution. In a previous study, a parameter named "paraxial estimator" was defined to check the validity of the paraxial approximation for avoiding obtaining the nonphysical solution of the paraxial equations, leading to a misinterpretation of the problem [8]. This paraxial estimator ($\tilde{\wp}$) is defined as the ratio of the propagation invariants of the Helmholtz and paraxial equations. Calculation of the paraxial estimator for any arbitrary field defined at any aperture plane $z = z_0$, can be done using expression defined in [9].

The paraxial estimator is the ratio of the true power crossing a transverse area obtained using the Helmholtz and paraxial equations, and if the paraxial approximation is valid, then the ratio must be unity. When the paraxial estimator goes below 1, the solution obtained using paraxial approximation becomes doubtful. It is reported that if the paraxial estimator value is less than 0.94, the solution of paraxial approximation without any correction is generally invalid [10]. Another important feature of the paraxial estimator is that it remains constant at different values of the propagation distances for free-space propagation if the field is not transformed by any external phase modifying structures such as lenses [10]. In the present study, we do not consider the effect of lenses, and thus, our calculation of the paraxial estimator is invariant of the propagation distances.

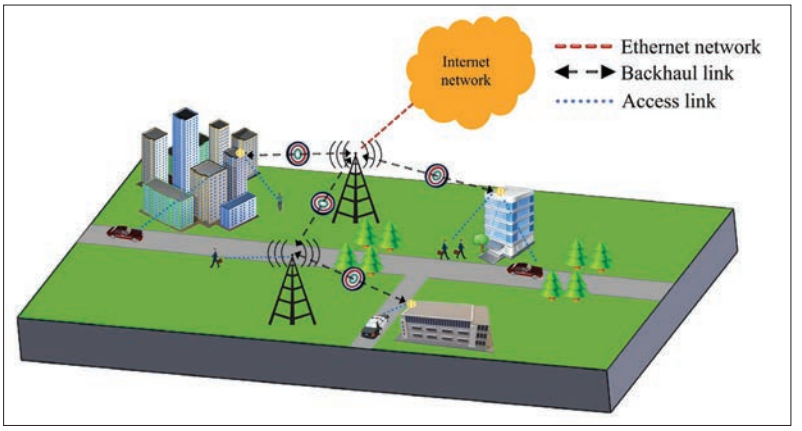

FIGURE 1. Backhaul wireless communication prototype based on OAM communication.

DoF Based on Paraxial Estimator

Considering that LG beams are the most common free-space OAM beams, in this section, we will analyze the DoF of the OAM channel with LG beams based on a paraxial estimator. This analysis has been carried out at the W-band in mm-wave frequency, although the results have been normalized with operating wavelength to generalize it for any frequency. The transmitter and receiver sizes are an important parameter for determining the DoF in case of nonparaxial or highly diverging beams, such as LG beams. A paraxial estimator, as discussed in the previous section, shows not only the validity of paraxial approximation but also the beam divergence: a lower value of the paraxial estimator leads to a higher divergence angle of the field.

Figures 2a and 2b show the paraxial estimator for the different-order LG beams with different beam waist radii. If the beam energy remains fixed during propagation, calculation of the paraxial estimator is only performed at the $z = 0$ transverse plane by solving field equations for different-order LG modes, because it is a propagation invariant. The paraxial estimator, which is a quality indicator of paraxiality, reduces for higher-order LG modes, as shown in Figs. 2a and 2b. The higher-order LG modes that diverge very quickly have a lower paraxial estimator, that is, they do not follow paraxial approximation.

The DoF of a wireless communication channel is considered as the maximum number of independent signals that can be simultaneously transmitted for unit bandwidth. In the case of OAM wireless communication, DoF can be defined as the total number of OAM modes that can be transmitted on a wireless channel to carry the information signals. In the case of a practical system, DoF is usually limited by the transmitter size, receiver size, and propagation distance. The receiver for an OAM wireless communication channel can be of different types, such as a mode sorter [11] or any UCA antenna [12]. Mode sorter-type receivers are aperture antennas that are required to receive complete energy of the transmitted beam at the receiver position. In this case, the receiver size must be greater than the beam radius of the LG beam. The analytic expression for the beam radius $W_p^l(z)$ of the LG beams [13] and its relation to the paraxial estimator leads us to the definition of DoF which is reliant on paraxial estimator.

In the case of OAM wireless communication, DoF can be defined as the total number of OAM modes that can be transmitted on a wireless channel to carry the information signals. In the case of a practical system, DoF is usually limited by the transmitter size, receiver size, and propagation distance.

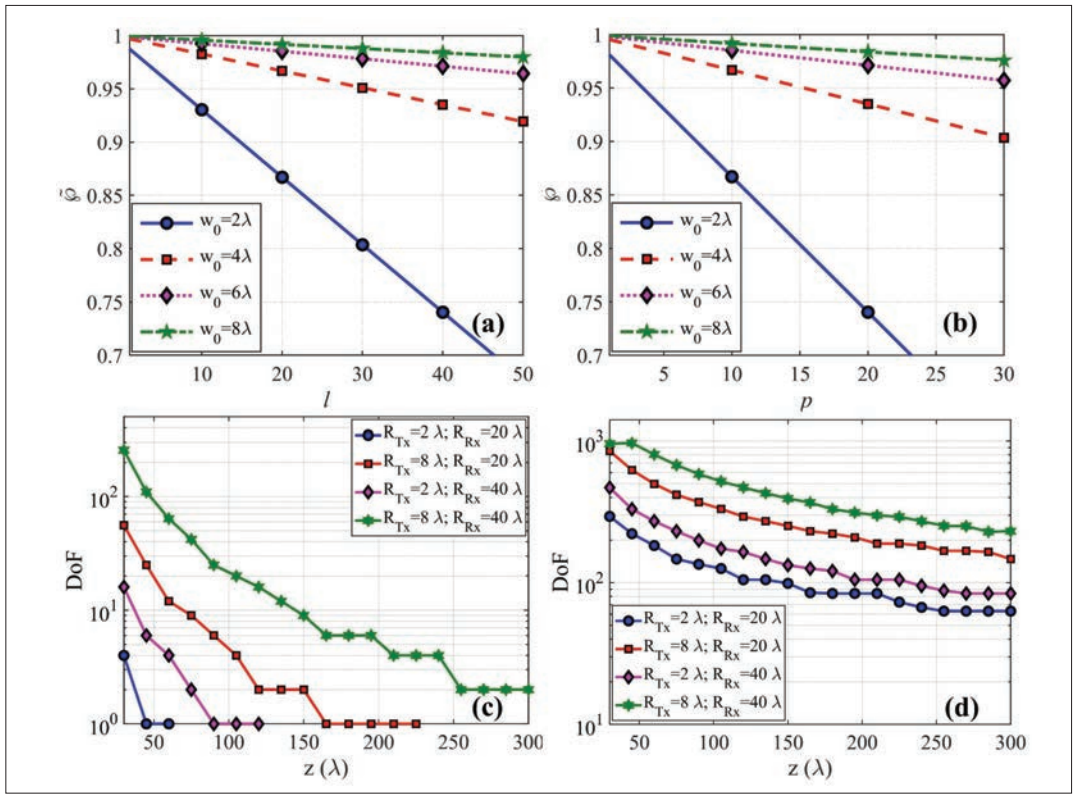

FIGURE 2. Paraxial estimator vs. a) azimuthal index (l) for $LG_{0,l}$ beam; b) radial index (p) for $LG_{p,0}$ beams with different beam waist radii. Calculated DoF of the OAM wireless communication link at different propagation distances with fixed transmitter and receiver sizes for c) aperture based receiver configuration; d) detector employed receiver configuration.

DoF for the wireless communication setup is defined as

$$DoF(z) \triangleq \max_{w_p^l(0)} \#\left\{ LG_p^l \middle| \bar{\wp}_p^l \geq 1 - \frac{R_{Rx}^2(z)}{4(z^2+z_R^2}, R_{Tx} \geq W_p^l(0) \right\}, \quad (1)$$

where $W_p^l(0)$ is the initial beam waist radius and $\bar{\wp}_p^l$ is the paraxial estimator of the LG$_{(p,l)}$ beam, z_R is the Rayleigh length, R_{Rx} is the receiver radius, R_{Tx} denotes the transmitter radius and $\#\{.\}$ represents the size of the set. If the condition based on the paraxial estimator defined in Eq. 1 is maintained for a particular LG mode, then its beam radius at the receiver location will be smaller than the size of the receiver. Additionally, we also put a constraint in Eq. 1 that transmitter size should be greater than the initial beam waist radius of the mode. We calculate the maximum number of possible LG modes that satisfy these conditions to determine the DoF of the channel.

Figure 2c shows the DoF value calculated based on Eq. 1 for different propagation distances at fixed transmitter and receiver sizes. The calculation is performed by considering that the beam waist radius of the modes is equal to the maximum possible value, that is, equal to the transmitter radius. A larger beam waist radius of the mode leads to a lower divergence angle, which indicates that the calculated DoF is the maximum value for the specific configuration of the receiver. Generated DoF results are for only one rotation and one polarization OAM modes. If we consider both rotations and both polarization modes, then the DoF will multiply four times.

Another configuration of the OAM receiver is based on the detector probe antenna, where different probes are placed at different azimuthal positions of the annular rings. These probe antennas are usually Schottky detectors or patch antennas, which measure the field amplitude at a fixed azimuthal position to determine the OAM mode. Detection of the OAM modes in this case is restricted by the dynamic range of the detectors. Higher-order LG modes diverge quickly, and their power is distributed on a large beam area at the receiver plane. The detectors placed at a radial position receive a fraction of this power depending upon the mode index and the detector position.

Owing to the divergence of higher-order LG modes, their power density decreases sequentially if the total power of each LG beam is the same. If we consider that the detector is placed on the radial maxima of the LG$_{0,1}$ mode, then that detector will be offset from the radial maxima position for other higher-order modes. This will cause a difference in the received power signal for different higher-order modes. In this case, the detection of the LG modes is restricted by the dynamic range of the detectors. For millimeter-wave detectors, the nominal value of the dynamic range is approximately −40 dB. The DoF for this configuration is calculated by evaluating the field pattern of each mode at the receiver position. The receiver is assumed to be placed at a radial position (R_{ring}) to capture the amplitude of the radiated LG modes. The DoF is determined by calculating the number of modes whose reference amplitude with respect

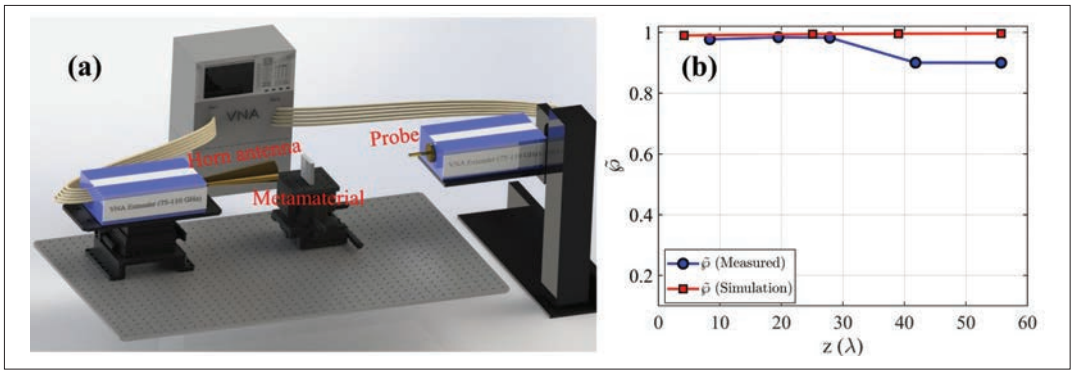

FIGURE 3. a) Measurement setup for the generated OAM beam using a metamaterial slab; b) measured and simulated paraxial estimator value of the generated $LG_{0,1}$ beam using a metamaterial slab at different distances.

to the $LG_{0,1}$ mode is greater than the assumed dynamic range of the receiver (–40 dB).

We consider that most of the beam power is contained within the area with beam radius W_p^l and the remaining power beyond it is neglected. Additionally, each LG beam has the same total power at the receiver location.

Power in the $LG_{p,l}$ beam at the receiver location is

$$P_{p,l}(R_{ring},z) = \frac{z_R^2}{z_R^2+z^2} 2x_{p,l}^2 \left[L_p^l\left(2x_{p,l}^2(z)\right)\exp\left(-x_{p,l}^2(z)\right)\right]^2 \quad (2)$$

where

$$x_{p,l}(z) = \frac{R_{ring}}{w_p^l(z)} = \frac{R_{ring}}{\sqrt{4(1-\bar{\wp})(z^2+z_R^2)}}$$

is the ratio of the receiver radial location to the total beam radius. Equation 2 is multiplied with the probe area to calculate the power received by the receiver placed at the radial position of $r = R_{ring}$. Figure 2d shows the calculated value of DoF based on the calculated power for different transmitter and receiver sizes. Comparing the values of DoF obtained from Figs. 2c and 2d, we conclude that receivers employing detectors have much higher DoF values.

Experimental Proof of Paraxial Estimator for LG Beams

To validate our point, we perform a proof-of-concept experiment for the evaluation of the paraxial estimator. The Gaussian beam emitted from a W-band Gaussian horn antenna connected to an Agilent Vector Network Analyzer (VNA) port is converted into the LG_{01} beam by a metamaterial slab placed 4 cm away from the antenna aperture and continues to propagate in free space. We measure the 2D electric field patterns at different axial distances of the generated OAM beam of order $l = 1$. The field pattern of the $LG_{0,1}$ beam is measured in the transverse plane at different z locations using an open-ended waveguide probe, which is connected to the other port of the VNA, as shown in Fig. 3a. The paraxial estimator $\tilde{\wp}(z)$ in the generated LG_{01} beam is calculated based on field measurement. The results, along with the simulation results obtained with the CST microwave studio 2019, are shown in Fig. 3b.

In the simulation, the paraxiality estimator of the $l = 1$ beam remains almost constant with the propagation distance. The overall simulation results agree well with the measurement, although one can notice that the measurement results show a significant change in the paraxial estimator beyond $z = 150$ mm (42.6λ), which is due to the limited size of the measurement plane. We observe that a major side lobe of the electric field is at the boundary of the measurement plane and is not completely retrieved inside the measurement plane, due to which the paraxial estimator is reduced.

Orthogonality

The orthogonality of the LG modes is an inherent quality for an efficient and high-speed wireless communication maintained during their propagation in a medium. Orthogonality in the LG modes is maintained between modes with different azimuthal indices, due to phase vorticity and modes with different radial indices, due to Laguerre polynomial dependency of the field profile in the radial direction. In a theoretical model, the orthogonality of LG modes is always maintained if the calculation domain is large enough to contain the complete energy of the system until their field profile is not tampered. However, in a practical system, where the transmitter and receiver sizes are finite and the beam truncation can occur due to the finite receiver size, the radial index orthogonality is an essential parameter to study. Azimuthal index-based orthogonality is maintained even for this truncated beam.

In the previous section, we considered that the receiver and transmitter sizes must be greater than the beam radius of the $LG_{p,l}$ beam, to determine the DoF of the channel. If the receiver and transmitter sizes are smaller than the beam radius, then the orthogonality between the received truncated LG modes worsens. This can be quantitatively explained by calculating the orthogonality coefficient between the truncated field of the received mode pair $LG_{p,l}$ and $LG_{p+1,l}$ mode, and can be calculated as [7]

$$\mu[p,p+1] = 1 - \frac{\int_0^{2\pi}\int_0^{w_z^{p,l}} u_{p,l}U_{p+1,l}^* r dr d\phi}{\int_0^{2\pi}\int_0^{w_z^{p,l}} |u_{p,l}|^2 r dr d\phi \int_0^{2\pi}\int_0^{w_z^{p,l}} |U_{p+1,l}^*|^2 r dr d\phi} \quad (3)$$

The value of the orthogonality coefficient (μ) should be one in an ideal case. However, in the case of a truncated beam, the value is not exactly one and starts to decrease when the ratio of the

The orthogonality of the LG modes is an inherent quality for an efficient and high-speed wireless communication maintained during their propagation in a medium. Orthogonality in the LG modes is maintained between modes with different azimuthal indices, due to phase vorticity and modes with different radial indices, due to Laguerre polynomial dependency of the field profile in the radial direction.

The value of the orthogonality coefficient (μ) should be one in an ideal case. However, in the case of a truncated beam, the value is not exactly one and starts to decrease when the ratio of the beam size and receiver size increases, that is, the orthogonality condition is vanishing and a larger crosstalk can be observed between multiple modes during wireless transmission.

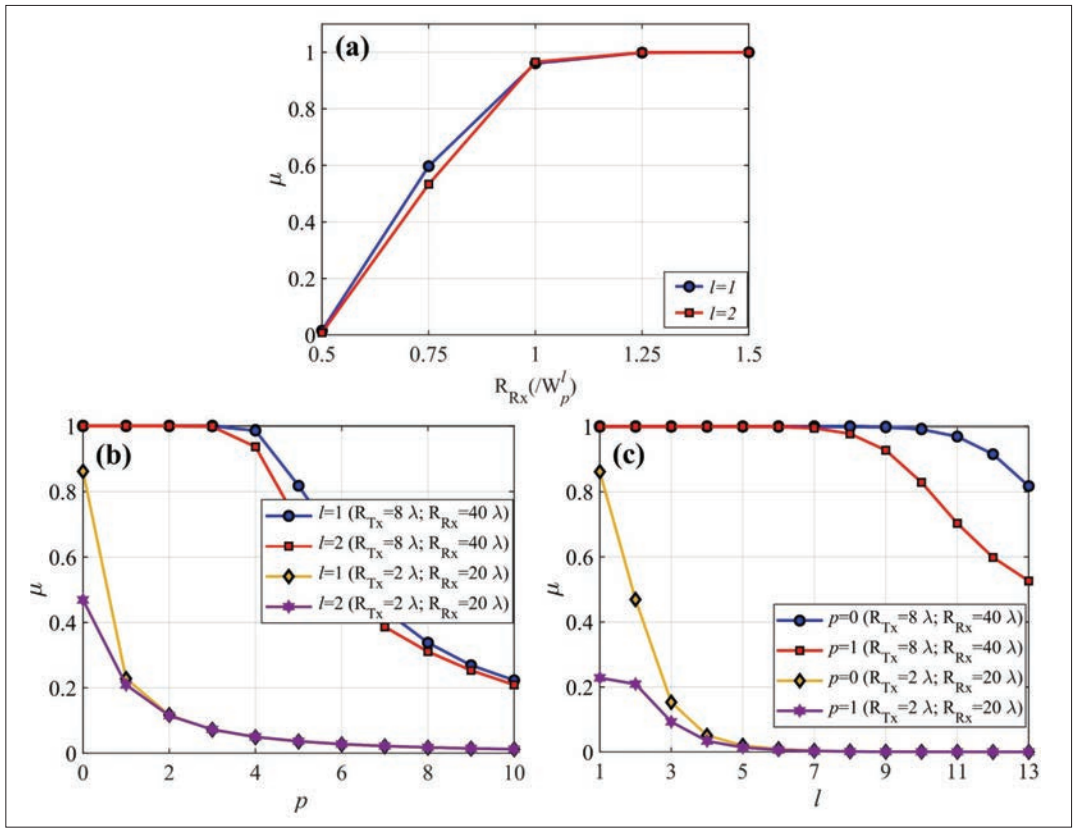

FIGURE 4. Orthogonality parameter (μ) calculated between: a) $LG_{0,l}$ and $LG_{1,l}$ modes for l =1,2 at different receiver sizes; b) $LG_{p,l}$ and $LG_{p+1,l}$ modes for different values of p; c) $LG_{p,l}$ and $LG_{p+1,l}$ modes for different values of l at fixed transmitter and receiver sizes.

beam size and receiver size increases, that is, the orthogonality condition is vanishing and a larger crosstalk can be observed between multiple modes during wireless transmission.

Figure 4a shows the orthogonality between the LG modes with radial index variation, for a receiver placed at 300λ with fixed transmitter and different receiver sizes. As the receiver size is smaller than the beam radius at the receiver location for a particular LG mode, its orthogonality parameter starts to diminish. The acceptable limit of the orthogonality parameter for our further calculation is decided to be the same as the value for the $LG_{0,1}$ beam when the receiver size is the same as the size of the $LG_{0,1}$ beam, which is 0.97. It determines the validity of the mode transmission based on orthogonality. Figure 4(b) shows the variation in the orthogonality parameter for different p indices and l = 1, 2 indices. It shows that, for the l = 1 index, the maximum possible modes that follow orthogonality have radial index 4, while for l = 2, the radial index reduces to 3 for transmitter and receiver sizes of 8λ and 40λ, respectively.

Similarly, Fig. 4c shows the variation in the orthogonality parameter for different l indices at radial indices of 0 and 1. Here, the orthogonality for the mode pair with radial indices p = 0, 1 and p = 1, 2 is maintained up to l = 11 and 8 indices, respectively, for transmitter size of 8λ and receiver size of 40λ.

Paraxial Estimator for TE Modes in Free Space

In this section, we will study the phenomenon of OAM property of the circular $TE_{m,n}$ mode radiated to free space. Circular $TE_{m,n}$ modes are similar to the $LG_{p,l}$ beams in terms of helical phase front and follow orthogonality in a guided transmission. These modes are naturally confined inside a metallic circular waveguide and are highly divergent after being launched into free space from the metallic waveguide aperture. Depending upon the launching waveguide aperture, the divergence of the radiated $TE_{m,n}$ modes differs, which can also be represented in terms of its paraxial estimator. Figures 5a and 5b present the summarized results of the paraxial estimator for different $TE_{m,n}$ modes radiated from different waveguide radii. These results are obtained using a field profile generated in Surf3d simulations. Surf3d is a commercially available software, which generates the electric field information of any arbitrary $TE_{m,n}$ mode radiating from a waveguide aperture at any given distance from the source by solving electric field integral equations (EFIEs) [14]. A larger waveguide radius leads to a higher paraxial estimator of the $TE_{m,n}$ mode. Compared to the $LG_{p,l}$ modes, the paraxial estimator of the $TE_{m,n}$ modes reduce rapidly for higher-order modes because these beams exhibit high divergence property and follow nonparaxiality.

To demonstrate the validity of our simulation result, we calculate the paraxial estimator of a radiated $TE_{6,2}$ mode from a $TE_{6,2}$ mode generator that is available in use in the laboratory. The detailed information on the mode generator design can be found in [15]. The mode generator generates the $TE_{6,2}$ mode at 95 GHz frequency. One port of the VNA is connected to the input waveguide port, while the other is connected to the open-ended waveguide probe, which is mounted on a two-di-

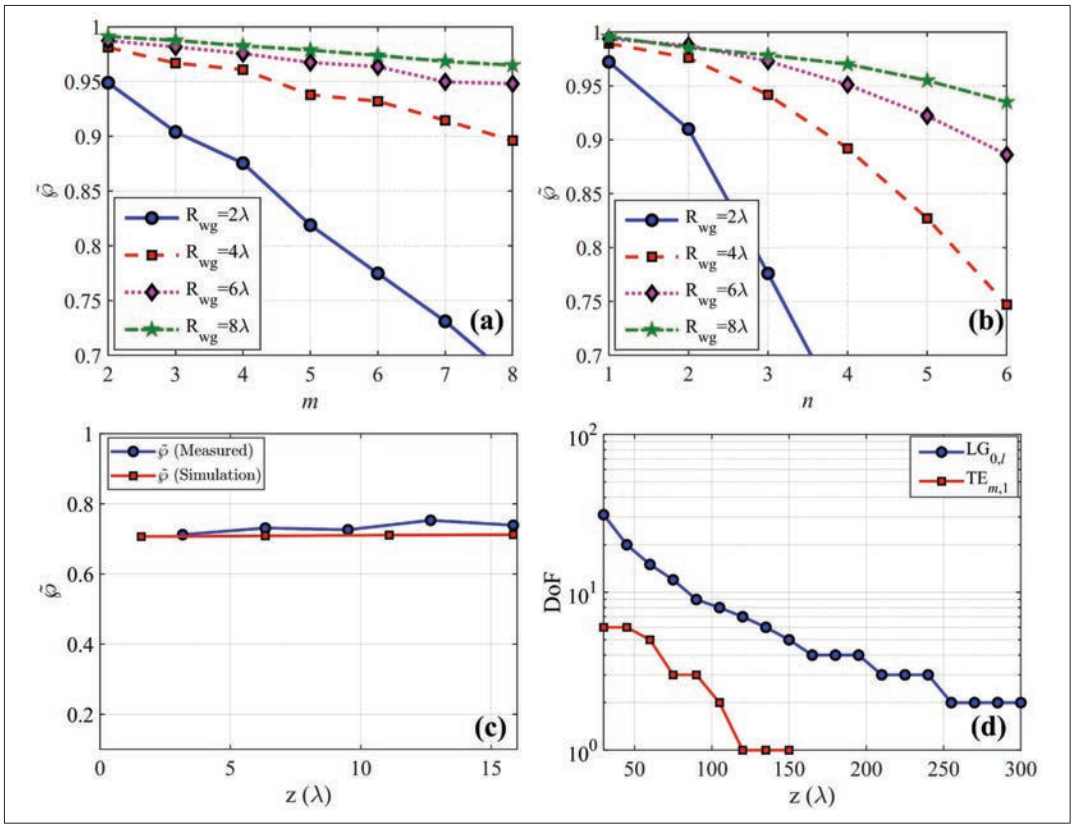

FIGURE 5. Paraxial estimator vs. a) azimuthal index (m) for $TE_{m,1}$ beam; b) radial index (n) for $TE_{1,n}$ beams with different waveguide radii; c) paraxial estimator of the generated $TE_{6,2}$ mode using the mode generator; d) comparison of DoF for $TE_{m,1}$ and $LG_{0,l}$ based wireless communication link with a transmitter size of 8λ and receiver size of 40λ.

mensional translational stage, similar to the setup shown in Fig. 3a. This assembly can measure both orthogonal polarizations of the electric field at a distance from the waveguide aperture of the mode generator. The measurement of the electric field at different transverse planes is conducted. Figure 5c shows the value of the calculated paraxial estimator from the measured electric field patterns at different axial distances from the aperture. The value of the paraxial estimator of the radiated $TE_{6,2}$ mode is approximately 0.72, which indicates a higher divergence angle of the radiated mode. This divergence angle is dependent upon the mode index and the aperture of the waveguide. The measurement and simulation results are consistent and confirm that the paraxial estimator of the radiated mode is low, which is a measure of its higher divergence angle.

Calculation of the DoF based on the paraxial estimator for TE beams is not as straightforward as that for LG beams, because there is no explicit relation of the beam radius of the TE modes propagating in free space. Beam radius expansion of the TE mode radiated from metallic waveguide aperture can be calculated from its free space field profile obtained using the Surf3d simulation tool. By applying linear fitting to the beam radius expansion in the propagation direction, the asymptotic growth angle is calculated. The DoF of the channel for TE mode transmission is determined in a similar fashion as LG modes by considering that the receiver radius must be greater than the beam radius of the candidate modes at the receiver position.

Now, from the data provided in Fig. 5a and from Surf3d simulation results, we calculate the DoF for the $TE_{m,1}$ modes for R_{Tx} = 8λ and R_{Rx} = 40λ and compare it with the $LG_{0,l}$ modes in Fig. 5d. The maximum permissible distance for communication using the $TE_{m,1}$ mode is 150λ for this receiver configuration, while at this distance, the DoF of the LG beam-based wireless communication setup is 5, as shown in Fig. 5d. For LG modes, the maximum permissible distance for this configuration is approximately 300λ. This comparison shows that TE modes cannot travel long distances but can be used for a small-distance communication setup. A further detailed study of the higher-order radial index TE modes and their effect on DoF is beyond the scope of this study. The orthogonality of the radiating TE modes is similar to that of the LG modes and can be maintained between different azimuthal index modes and different radial index modes. In the case of the truncated TE modes, the orthogonality for the radial index modes is altered.

Conclusions

We initiated this study to answer the question of infinite channel capacity for a practical OAM-based wireless communication link. Considering that the natural tendency of the generalized OAM beams (LG or TE beams) is to diverge, we focused on paraxiality. In more general terms, paraxial and nonparaxial beams differ based on their divergence properties. A paraxial estimator, which is used to quantify the paraxiality of a beam, also indicates its divergence angle. In our study, we found that the paraxial estimator of LG beams decreases for higher-order modes and can be a parameter for defining the channel capacity

By applying linear fitting to the beam radius expansion in the propagation direction, the asymptotic growth angle is calculated. The DoF of the channel for TE mode transmission is determined in a similar fashion as LG modes by considering that the receiver radius must be greater than the beam radius of the candidate modes at the receiver position.

We concluded that the DoF of a wireless communication link based on OAM beams is limited by its divergence and can be identified based on the paraxiality and orthogonality conditions. This novel technique is a generalized method of calculating the DoF of the wireless communication link which is limited by the divergence of the beam and physical size of the transmitter and receiver.

of an OAM wireless link. In particular, we considered the transmitter and receiver sizes in the calculation of DoF of the wireless communication channel based on the paraxiality estimator for different receiver configurations. The orthogonality property for LG beams was also investigated for the case of truncated beams when the receiver was smaller than the beam size and only received a fraction of the total power. Furthermore, we validated our proposed concept by extending the study of calculating the DoF based on the paraxial estimator for the radiating TE beams. From our study, we concluded that the DoF of the wireless communication link with a practical size of the transmitter and receiver is finite and decreases as the propagation distance increases and the possible propagation distance of the highly diverging TE beams is less compared to the conventional LG beam without any focusing elements.

We concluded that the DoF of a wireless communication link based on OAM beams is limited by its divergence and can be identified based on the paraxiality and orthogonality conditions. This novel technique is a generalized method of calculating the DoF of the wireless communication link which is limited by the divergence of the beam and physical size of the transmitter and receiver. Several parameters that affect the DoF in a practical wireless communication link include the transmitter size, receiver size, and propagation distance, and we reported their dependencies on the paraxial estimator. The effects of focusing elements, atmospheric turbulence, and scattering, which can alter the channel capacity, have not been considered in the present calculation and we considered them as the scope of further study.

Acknowledgment

This work was supported by the Samsung Research Funding Center of Samsung Electronics under project number SRFC-TB1803-01.

References

[1] L. Allen *et al.*, "Orbital Angular Momentum of Light and the Transformation of Laguerre-Gaussian Laser Modes," *Physical Review A*, vol. 45, no. 11, 1992, p. 8185.
[2] Y. Shen *et al.*, "Optical Vortices 30 Years On: OAM Manipulation from Topological Charge to Multiple Singularities," *Light: Science & Applications*, vol. 8, no. 1, 2019, pp. 1–29.
[3] U. Siddique *et al.*, "Wireless Backhauling of 5G Small Cells: Challenges and Solution Approaches," *IEEE Wireless Commun.*, vol. 22, no. 5, 2015, pp. 22–31.
[4] S. Li *et al.*, "Atmospheric Turbulence Compensation in Orbital Angular Momentum Communications: Advances and Perspectives," *Optics Commun.*, vol. 408, 2018, pp. 68–81.
[5] A. F. Morabito, L. Di Donato, and T. Isernia, "Orbital Angular Momentum Antennas: Understanding Actual Possibilities Through the Aperture Antennas Theory," *IEEE Antennas and Propagation Mag.*, vol. 60, no. 2, 2018, pp. 59–67.
[6] T. Hu *et al.*, "OFDM-OAM Modulation for Future Wireless Communications," *IEEE Access*, vol. 7, 2019, pp. 59114–25.
[7] J. Xu, "Degrees of Freedom of OAM-Based Line-of-Sight Radio Systems," *IEEE Trans. Antennas and Propagation*, vol. 65, no. 4, 2017, pp. 1996–2008.
[8] P. Vaveliuk, B. Ruiz, and A. Lencina, "Limits of the Paraxial Approximation in Laser Beams," *Optics Letters*, vol. 32, no. 8, 2007, pp. 927–29.
[9] P. Vaveliuk, "Quantifying the Paraxiality for Laser Beams from the M 2 Factor," *Optics Letters*, vol. 34, no. 3, 2009, pp. 340–42.
[10] P. Vaveliuk and O. Martinez-Matos, "Effect of ABCD Transformations on Beam Paraxiality," *Optics Express*, vol. 19, no. 27, 2011, pp. 25944–53.
[11] H. Huang *et al.*, "Mode Division Multiplexing Using an Orbital Angular Momentum Mode Sorter and MIMO-DSP over a Graded-Index Few-Mode Optical Fibre," *Scientific Reports*, vol. 5, no. 1, 2015, pp. 1–7.
[12] Z.-G. Guo and G.-M. Yang, "Radial Uniform Circular Antenna Array for Dual-Mode OAM Communication," *IEEE Antennas and Wireless Propagation Letters*, vol. 16, 2016, pp. 404–07.
[13] R. L. Phillips and L. C. Andrews, "Spot Size and Divergence for Laguerre Gaussian Beams of Any Order," *Applied Optics*, vol. 22, no. 5, 1983, pp. 643–44.
[14] J. Neilson, "Surf3d and LOT: Computer Codes for Design and Analysis of High-Performance QO Launchers in Gyrotrons," *Proc. Infrared and Millimeter Waves, Conference Digest of the 2004 Joint 29th Int'l. Conf. 2004 and 12th Int'l. Conf. Terahertz Electronics, 2004*, 2004: IEEE, pp. 667–68.
[15] I. Lee *et al.*, "Accurate Identification of Whispering Gallery Mode Patterns of Gyrotron with Stabilized Electro-Optic Imaging System," *Physics of Plasmas*, vol. 25, no. 1, 2018, p. 013116.

Biographies

Ashwini Sawant (ash1990@unist.ac.kr) received the B.E. degree in electronics and communication engineering from ITM, Gwalior, India, in 2010, the M.Tech. degree in RF and microwave engineering from IIT Roorkee, India, in 2013, and the Ph.D. degree in electrical engineering from Ulsan National Institute of Science and Technology (UNIST), Ulsan, South Korea in 2019. He is currently working as a post-doctoral researcher at the Terahertz Vacuum Electronics and Electrodynamics (TEE) group, UNIST. His current research interests include the design and development of high-power vacuum tube devices, harmonic operations in gyrotrons, phase retrieval techniques, metamaterial structures, and orbital angular momentum beams.

Ingeun Lee (ianlee85@unist.ac.kr) received the Ph.D. degree in electrical engineering from Ulsan National Institute of Science and Technology (UNIST), Ulsan, South Korea in 2019. He is currently working as a post-doctoral researcher at the Terahertz Vacuum Electronics and Electrodynamics (TEE) group, UNIST. His research interests include the development of terahertz vacuum electronics, precision processing technologies for vacuum electron devices, terahertz wireless power transfer, metamaterial structures, and millimeter wave and terahertz imaging applications.

Bang Chul Jung (bcjung@cnu.ac.kr) received the B.S. degree in electronics engineering from Ajou University, Suwon, Korea, in 2002, and the M.S4. and Ph.D degrees in electrical and computer engineering from Korea Advanced Institute of Science and Technology (KAIST), Daejeon, Korea, in 2004 and 2008, respectively. He was a senior researcher/research professor with KAIST Institute for Information Technology Convergence, Daejeon, Korea, from January 2009 to February 2010. From March 2010 to August 2015, he was a faculty of Gyeongsang National University, Tongyeong, Korea. He is currently a professor in the Dept. of EE, Chungnam National University, Daejeon, Korea. He has served as an associate editor for *IEEE Vehicular Technology Magazine* since May 2020. He was the recipient of the 5th IEEE Communication Society Asia-Pacic Outstanding Young Researcher Award in 2011, the KICS Haedong Young Scholar Award in 2015, and the 29th KOFST Science and Technology Best Paper Award in 2019. His research interests include wireless communications, statistical signal processing, information theory, interference management, radar signal processing, spectrum sharing, multiple antennas, multiple access techniques, radio resource management, machine learning, and deep learning.

EunMi Choi (emchoi@unist.ac.kr) received the B.S. degree in physics from Ewha Womans University, Seoul, South Korea, in 2000, the M.S. degree in physics from the Pohang University of Science and Technology (POSTECH), Pohang, South Korea, in 2002, and the Ph.D. in physics from Massachusetts Institute of Technology (MIT), Cambridge, MA, USA, in 2007. After her post-doctoral research at Brookhaven National Laboratory (BNL) in 2008, she joined the Department of Electrical Engineering at Ulsan National Institute of Science and Technology (UNIST) in 2010 as an assistant professor, where she has been an associate professor since 2014. She is leading the group of THz Vacuum Electronics and Applied Electromagnetic Lab (TEE Lab). Her research focuses on the development of high power millimeter and THz wave sources using vacuum electron devices and explores its applications including orbital angular momentum (OAM) communications for future 6G and beyond.